Lattice-vibration and spin-fluctuation effects on photoemission from ferromagnetic Ni

I. Delgadillo,* H. Gollisch, and R. Feder
Theoretische Festkörperphysik, Universität Duisburg, 47048 Duisburg, Germany
(Received 17 June 1994)

A realistic theoretical treatment of the influence of lattice vibrations on electronic structure and photoemission has been extended to ferromagnetic 3*d* metals by simultaneously including correlated fluctuations of local moments. Numerical applications to photoemission from Ni(110) yield, for temperatures from 121 K up to the Curie temperature, spectra in good agreement with experimental data. The phonon-induced lifetime broadening, which is inherent in these calculations, enhances the merging behavior between opposite-spin peaks with increasing temperature. Comparison with experiment implies a sizable short-range magnetic order near T_c.

I. INTRODUCTION

The temperature dependence of the spin-resolved electronic structure of 3*d* ferromagnets and its manifestation in spin- and angle-resolved photoemission have been the subject of a number of theoretical studies (cf. Refs. 1–5 and references therein), which achieved quite good agreement with experimental photoemission data. These studies concentrated on the intrinsically magnetic temperature dependence associated with spin fluctuations and took account of lattice vibrations only in simple ways, either by convoluting the spectra by an additional Gaussian or by using complex phase shifts in the calculation of the photoemission final state. In both cases, correlations between the atomic vibrations are neglected. These correlations were, however, found to be important in a recent investigation for a nonmagnetic 3*d* metal (Cu).[6] One can therefore expect that they will also play a role in ferromagnets.

In this work, we investigate the joint effect of spin fluctuations and correlated ion core vibrations on electronic structure and photoemission of 3*d* ferromagnets. In Sec. II, we outline a formalism which combines a fluctuating local-magnetic-moment method (cf. Refs. 1–4) with a treatment of correlated lattice vibrations.[6] Numerical results are presented in Sec. III for the case of Ni and compared with experimental photoemission data over a wide temperature range.

II. THEORY

Our formalism is based on the adiabatic approximation. Hence, the treatment of the electronic structure at a given finite temperature T consists of the following two main parts: first, the determination of static "snapshots" at T of the positions $\vec{R}_i$ of the ion cores, where i is a site index, and of their local magnetic moments $\vec{m}_i$; secondly, the calculation of the electronic properties for each of these configurations $\{\vec{R}_i, \vec{m}_i\}$ followed by an average over a sufficient number of them.

Since both lattice vibrations and spin fluctuations destroy the translational crystal symmetry and thus invalidate Bloch's theorem, we simulate the infinite system by a large cluster of N atoms with periodic boundary conditions. As described in detail in Ref. 6, sets of atomic positions $\vec{R}_i$ at temperature T are determined subject to an equal-time displacement correlation function consistent with experimental phonon spectra. Sets of local magnetic moments $\vec{m}_i$ associated with the ion cores at $\vec{R}_i$ are subsequently obtained by the free-energy minimization procedure described in Ref. 4, such that their average corresponds to the mean magnetization $M(T)$ and that there is a short-range magnetic order, which we characterize by a parameter Λ denoting the full width at half maximum (FWHM) of the spin-spin correlation function.

For each configuration $\{\vec{R}_i, \vec{m}_i\}$ at temperature T, the electronic structure is calculated in a nonrelativistic tight-binding scheme including s, p, and d orbitals. The Hamiltonian matrix elements $H_{ilms,i'l'm's'}$ between orbitals lms and $l'm's'$ on sites $\vec{R}_i$ and $\vec{R}_{i'}$ are expressed in the form

$$h_{ilm,i'l'm'}\delta_{ss'} - \tfrac{1}{2}\hbar(\vec{\sigma}\cdot\vec{\Delta}_{ilm})_{ss'}\delta_{ii'}\delta_{ll'}\delta_{mm'}, \qquad (1)$$

where $\vec{\sigma}$ is the Pauli spin matrix vector and $\vec{\Delta}_{ilm}$ the local exchange field at site $\vec{R}_i$ corresponding to the local moment $\vec{m}_i$. Within the two-center approximation, the spin-independent first term can be written as (cf. Refs. 7 and 8)

$$h_{ilm,i'l'm'} = \sum_{\tilde{m}} S(lm,l'm',\tilde{m};\vec{R}_i-\vec{R}_{i'})V_{ll'\tilde{m}}(|\vec{R}_i-\vec{R}_{i'}|), \qquad (2)$$

where the direction-dependent Slater-Koster coefficients $S(\cdots)$ can be directly calculated in the usual way. To obtain the tight-binding parameters $V_{ll'\tilde{m}}$, which depend on the distance between the vibrationally displaced sites, we first determine the usual tight-binding parameters $V_{ll'\tilde{m}}(|\vec{R}_i^0-\vec{R}_{i'}^0|)$ for the equilibrium configuration $\{\vec{R}_i^0\}$ by means of a tight-binding fit to a first-principles band structure. Subsequently, we employ the scaling relation[9]

$$V_{ll'\tilde{m}}(|\vec{R}_i - \vec{R}_{i'}|) = \left\{ \frac{|\vec{R}_i^0 - \vec{R}_{i'}^0|}{|\vec{R}_i - \vec{R}_{i'}|} \right\}^{\kappa} V_{ll'\tilde{m}}(|\vec{R}_i^0 - \vec{R}_{i'}^0|), \tag{3}$$

where the exponent κ is 5, 7/2, and 2 for the (d,d), (d,sp) and (sp,sp) parameters, respectively.

From the Hamiltonian matrix elements defined by Eqs. (1)–(3), the total and $\vec{k}$-resolved spin-dependent electronic densities are obtained by evaluating the appropriate diagonal Green function matrix elements by means of Haydock's recursion scheme[10] and subsequently averaging over the configurations $\{\vec{R}_i, \vec{m}_i\}$. For photoemission, we employ a bulk interband transition model. Following Ref. 11, the photocurrent in the direction $\vec{k}$ is obtained as the diagonal element of the initial-state Green function with respect to the state $\vec{A} \cdot \vec{p}|\vec{k}\rangle$, where $\vec{A}$ is the magnetic vector potential of the photon field, $\vec{p}$ the momentum operator, and $|\vec{k}\rangle$ a bulk final state. Strictly, the latter should also be calculated for the individual configurations, but since its damping is dominated by electron-electron processes and since the exchange splitting decreases with increasing electron energy we choose to ignore at present its modification by lattice vibrations and spin fluctuations.

For the computational application to Ni, we adopt the following model specifications. For the Hamiltonian matrix elements [Eq. (1)] at $T = 0$, a first choice results from a tight-binding fit to a band structure obtained from first principles by self-consistent linear muffin-tin orbital (LMTO) calculation. The magnitude of the local exchange field Δ is then 0.57 eV for all lm, corresponding to a uniform exchange splitting of the $T = 0$ majority and minority spin bands by this amount. As is well known, this is, because of correlation and self-energy effects, at variance with the (quasi-particle) exchange splitting observed in photoemission experiments, which is first much smaller and secondly symmetry dependent. For our photoemission calculations we therefore adopt values consistent with experimental band structures at low temperature: $\Delta = 0$ for s and p orbitals, and 0.188 and 0.326 eV for e_g and t_{2g} d orbitals, respectively. For finite temperature, the magnitudes of these local exchange splittings are retained constant and their directions fluctuate subject to the mean magnetization $M(T)$ and our short-range-order parameter Λ, which is adjustable to match experiment.

The phonon dispersion relations $\omega_{\vec{q}j}$, which are required as input for the atomic displacement correlation function, are obtained from the usual harmonic-approximation dynamical matrix after modeling the force constant matrix empirically from elastic constants.[12] Anharmonic effects are approximately taken into account in the "quasiharmonic approximation" as follows. For a given T, the set $\{\vec{R}_i^0\}$ is taken as the equilibrium configuration of the thermally expanded lattice at T. Phonon spectra and thence displacement configurations are calculated on the basis of elastic constants appropriate for this T. The cubic clusters are taken to consist of $4 \times 8^3 = 2048$ atoms. The number of configurations found sufficient for convergence is typically 5.

Hole lifetime effects are easily incorporated in the recursion calculations via an imaginary self-energy part, which leads to a Lorentzian broadening of the spectra. Physically, the hole lifetime is determined by electron-hole, electron-magnon, and electron-phonon scattering. Since the latter two mechanisms are already inherent in our adiabatic-approximation approach, we explicitly represent only the first one by an imaginary self-energy part, for which we choose the spin-independent form $2E^2/(E^2 + 4)$ eV with energy E relative to the Fermi energy (as in Ref. 2).

III. NUMERICAL RESULTS AND COMPARISON WITH EXPERIMENT

The influence of lattice vibrations and spin fluctuations on the Bloch spectral function $\mathrm{Im}G(E,\vec{k})$ for ferromagnetic Ni is illustrated in Fig. 1 by typical results obtained for the majority and minority spin Δ_5 bands at $\vec{k} = 0.6$ along Γ-X. In the bottom panels, we show the (nonrelativistic) band structure first as obtained in self-consistent local-spin-density approximation (LSDA) calculations, with a constant exchange splitting $\Delta_{\mathrm{ex}} = 0.57$ eV, and secondly with a k- and symmetry-dependent Δ_{ex} with values between 0.18 and 0.33 eV (cf. Ref. 2) corresponding to the experimentally observed quasiparticles. The spectral function at $T = 0$ is indicated by the dashed vertical lines. For $T_c = 630$ K, we first consider the hypothetical case that lattice vibrations are fully present, while magnetically the ground state persists. The spectral function peaks (in the curves labeled "P" for phonons) are seen to be shifted and asymmetrically broadened, with a FWHM of about 0.2 eV for both majority and minority spin. This width reflects the electron-phonon contribution to the imaginary electron self-energy part. If the correlations between the atomic vibrations are neglected (dashed curves "P"), the peaks are broader and more strongly shifted. As one would expect, these findings are the same as our earlier ones for Cu.[6]

The effect of spin fluctuations in the absence of lattice vibrations is demonstrated by the spectra at T_c labelled "S" for several values of the magnetic short-range-order parameter Λ. In the case of $\Delta_{\mathrm{ex}} = 0.57$ eV (left-hand panel), the fairly large short-range order of $\Lambda = 12$ Å leads to two distinct peaks separated by a reduced apparent exchange splitting, whereas in the disordered-local-moment limit $\Lambda = 0$ the two peaks merge into one located halfway in between. For the smaller Δ_{ex} (right-hand panel), the $\Lambda = 12$ Å peaks appear already "merged" as much as the $\Lambda = 8$ Å ones for $\Delta_{ex} = 0.57$ eV. Such Δ_{ex} dependence of the short-range-order influence has already been reported earlier.[2] Taking into account both lattice vibrations and spin fluctuations, we obtain the spectral functions labeled "S and P" (in Fig. 1). For $\Lambda = 0$, there is again one central peak, which, compared to its "S" counterpart, is shifted and asymmetrically broadened just like the "P" peaks relative to the $T = 0$ spectral function. For the nonzero Λ values, the separate peaks obtained for "S" only are

now merged into a single broad peak with its center of gravity moving slightly to the left with increasing Λ. For the smaller Δ_{ex}, the $\Lambda = 12$ Å result is now rather similar to the one for $\Lambda = 0$, i.e., the manifestation of magnetic short-range order is obscured by the lattice vibrations.

Since very detailed temperature-dependent photoemission data are available for ferromagnetic Ni(110),[13,14] we now focus on this surface. As a prerequisite, we show in Fig. 2 the bulk band structure along $K(S)X$ for our symmetry-dependent Δ_{ex} model, which reproduces the experimental $\Delta_{ex} = 0.18$ eV of the S_4 spin doublet near X. According to nonrelativistic dipole selection rules, electrons from S_4 initial states are excited in normal photoemission by s-polarized light with the electric field vector parallel to the $[1\bar{1}0]$ direction. The calculated $T = 0$ normal photoemission spectra in Fig. 2 illustrate the influence of our energy-dependent hole lifetime (i.e., a Lorentzian broadening) and its superposition by a Gaussian of 0.1 eV FWHM corresponding to the experimental energy resolution in Refs. 13 and 14. The following finite-T spectra all include both broadenings.

In Fig. 3 we present spin-resolved photoemission spectra, which evolve from the above S_4 doublet (at $T = 0$) with increasing T. First consider the effect of spin fluctuations in the absence of lattice vibrations (left-hand column of Fig. 3). At room temperature and below, the majority spin peak is lower and broader than the minority one, because the inverse hole lifetime increases away from the Fermi energy. As T increases, the majority peak is rather strongly further broadened and shifted towards the minority peak, whereas the minority peak is only slightly broadened and shifted. Such different temperature dependence has been found earlier for emission from H'_{25} states in Fe(001).[1] As has been been explained in detail, it is characteristic for states near the top of a spin-split band, where the minority spin electrons are scattered by the magnetic disorder into opposite-spin states more weakly than the majority spin electrons.

Due to lattice vibrations, both peaks experience, as one naively expects, a further broadening, which increases with temperature (see central panel of Fig. 3). It is, however, remarkable that the minority peak is affected more strongly than the majority peak. This may be understood from the fact, already suggested by the $T = 0$ band structure in Fig. 2, that at energies near the minority peak there is a higher density of states, which entails a

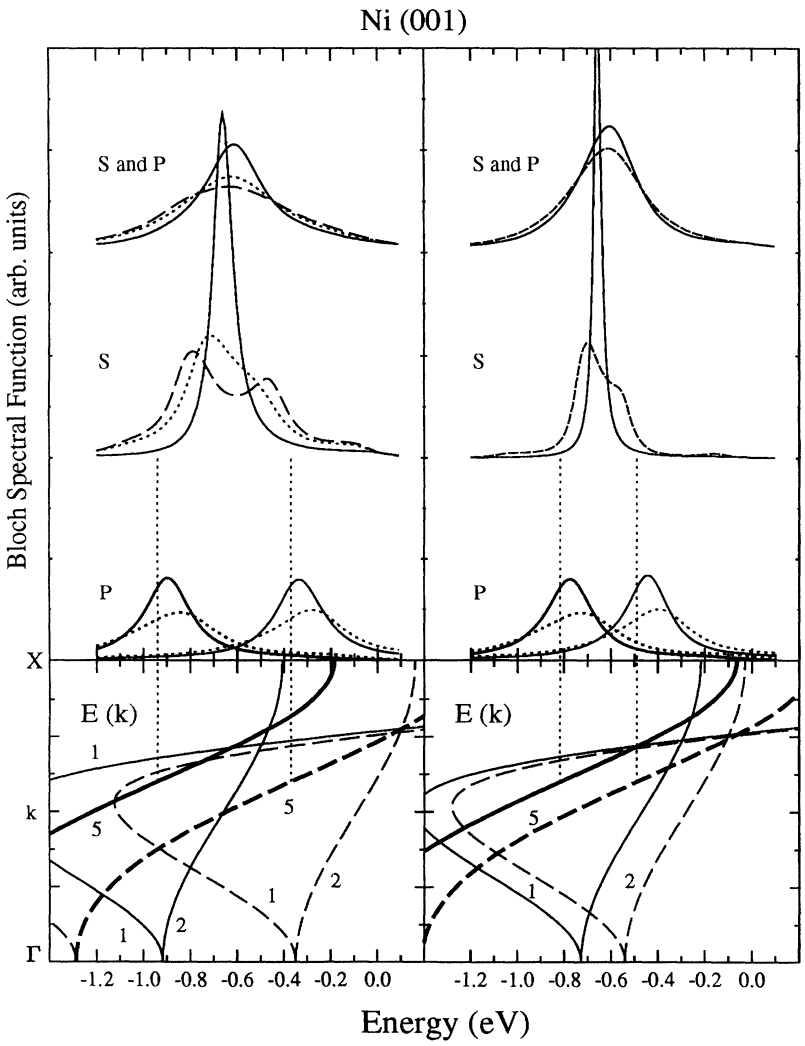

FIG. 1. Bloch spectral function of ferromagnetic Ni at T_c for $\vec{k} = 0.6$ (Γ-X) taking into account correlated and uncorrelated lattice vibrations only (solid and dashed curves labeled "P" for phonons), spin fluctuations only (curves "S"), and spin fluctuations and correlated lattice vibrations simultaneously (curves "S and P"); in the latter two cases, the short-range order parameter Λ is 0 (solid lines), 8 Å (short-dashed lines), and 12 Å (long-dashed lines). The vertical short-dashed lines indicate the spectral function at $T = 0$. In the (nonrelativistic) band structure (bottom panels), the majority (solid lines) and minority (dashed lines) bands are labeled by the corresponding single-group representations ("5" for Δ_5, etc.). The energy zero is the Fermi energy. In the left-hand part of the figure, the exchange splitting is 0.57 eV; in the right-hand part it is k and symmetry dependent (with values between 0.18 and 0.33 eV).

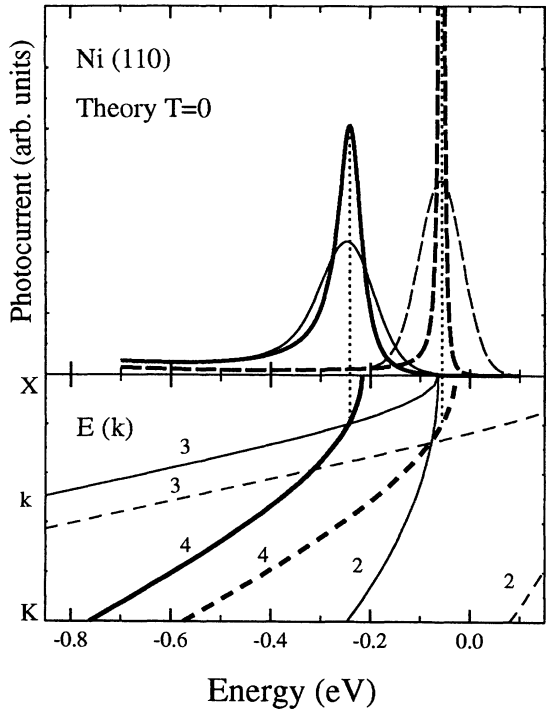

FIG. 2. Calculated *spin-resolved* normal photoemission spectra from Ni(110) at $T = 0$ by 16.85 eV photons with $\vec{E}$ parallel to $[1\bar{1}0]$, and band structure along $K(S)X$ (with labels indicating the single-group representations S_i). The majority (solid lines) and minority (dashed lines) spectra include a hole-lifetime Lorentzian (thick lines) and this Lorentzian together with a Gaussian of 0.1 eV FWHM (thin lines).

higher electron-phonon scattering rate. Comparing with experiment[13] (right-hand column of Fig. 3), it is obvious that the spectra calculated with lattice vibrations agree significantly better than those obtained with spin fluctuations only. The $0.9T_c$ spectra suggest a preference of a short-range order of about $\Lambda = 8$ Å.

A comparison with spin-averaged experimental photoemission spectra,[14] which extend over a wider temperature range, is shown in Fig. 4. At all temperatures, these data are in very good agreement with the theoretical spectra, which include lattice-vibration effects. At the lower temperatures (going from 121 to 362 K), spin fluctuations are seen to play almost no role, while lattice vibrations shift both peaks towards higher energy and reduce the height of the minority peak relative to the majority peak. At higher temperatures, spin fluctuations cause the peaks to move towards each other, and the right shift of the minority peak due to lattice vibrations is more than compensated. The influence of short-range magnetic order at T_c, which is quite pronounced in the calculated "spin-fluctuation-only" spectra, is seen to be strongly reduced by the lattice vibrations. Comparison with the experimental data appears to slightly favor a finite short-range order, with a rough estimate of Λ somewhere between about 6 and 14 Å.

The extent to which simpler approximations of phonon effects on photoemission spectra might suffice is demonstrated in Fig. 5. The top curve "no phonons" involves only spin fluctuations. The simplest simulation by a Gaussian of 0.05 eV is seen to fail to reduce the minority peak sufficiently compared to the experimental data. Choosing this Gaussian larger would make both peaks

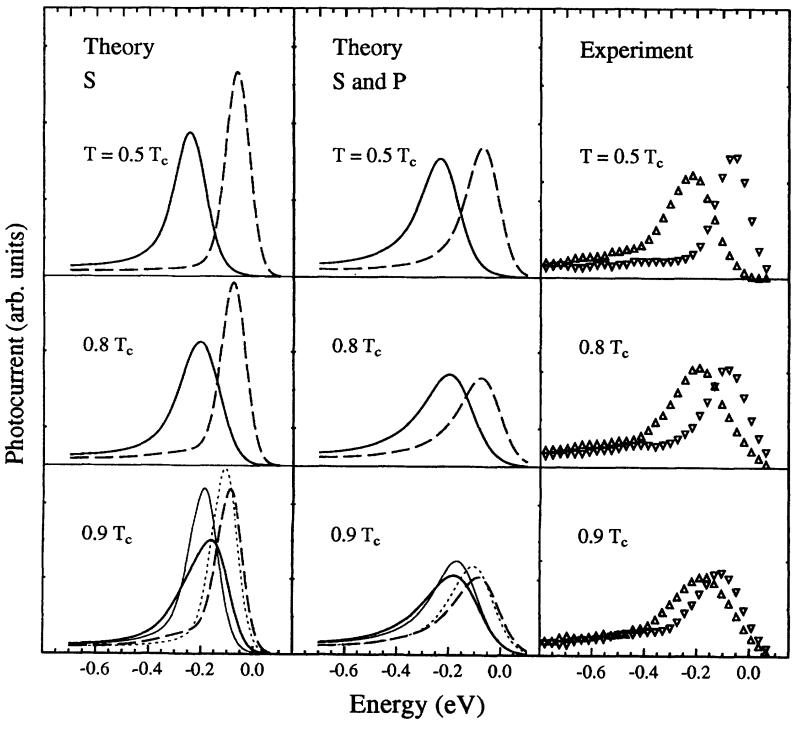

FIG. 3. *Spin-resolved* normal photoemission from Ni(110) by 16.85 eV photons with $\vec{E}$ parallel to $[1\bar{1}0]$ at temperatures (relative to T_c) as indicated: Theory for magnetic short-range order $\Lambda = 8$ Å (thick lines) and 0 (thin lines) including only spin fluctuations (left-hand column) and spin fluctuations together with phonons (central column) in comparison with experimental data from Ref. 13 (right-hand column). All calculated spectra have been convoluted by a Gaussian of 0.1 eV FWHM corresponding to the experimental energy resolution.

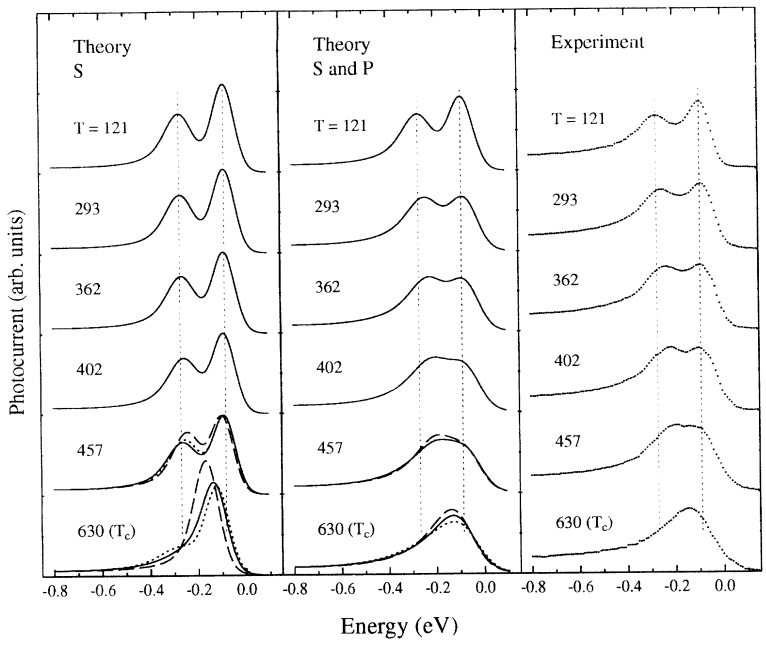

FIG. 4. As Fig. 3, but *spin-integrated* spectra (at temperatures given in K) compared with experimental data Ref. 14. The theoretical spectra were obtained for short-range order $\Lambda = 8$ Å (solid lines), 12 Å (dotted lines), and 0 (dashed lines).

too broad. Neglecting in our method the correlations between the atomic vibrations, we obtain the curve labeled "phonons uncorrelated." It is seen to match experiment better than the Gaussian convolution, but clearly less well than the spectrum including correlations.

IV. CONCLUSION

Our calculations of normal photoemission spectra for ferromagnetic Ni(110) have shown that the inclusion of correlated lattice vibrations, in addition to spin fluctuations, leads to a consistently good agreement with experimental data over a wide range of temperatures. This level of agreement cannot be obtained if phonon effects are completely ignored or treated in simpler approximations. In particular, the second-best approximation involving uncorrelated atomic vibrations, which we have employed in additional test calculations and which is inherent in the use of imaginary scattering phase shift contributions in layer Korringa-Kohn-Rostoker (KKR) photoemission formalisms, still produces discernible discrepancies with experiment, which are removed by taking into account vibrational correlations.

As a consequence of lattice vibrations, the sensitivity of calculated spectra near and at T_c to the amount of short-range magnetic order is substantially reduced in the case of Ni, where the contribution of the electron-phonon interaction to lifetime broadening, for which we obtain 0.182 eV near T_c, is almost the same as the magnetic exchange splitting of the S_4 bands and comparable to the maximal Δ_{ex} of 0.33 eV. Our comparison with experimental data still suggests a substantial short-range order, but its extent can only be broadly estimated to be

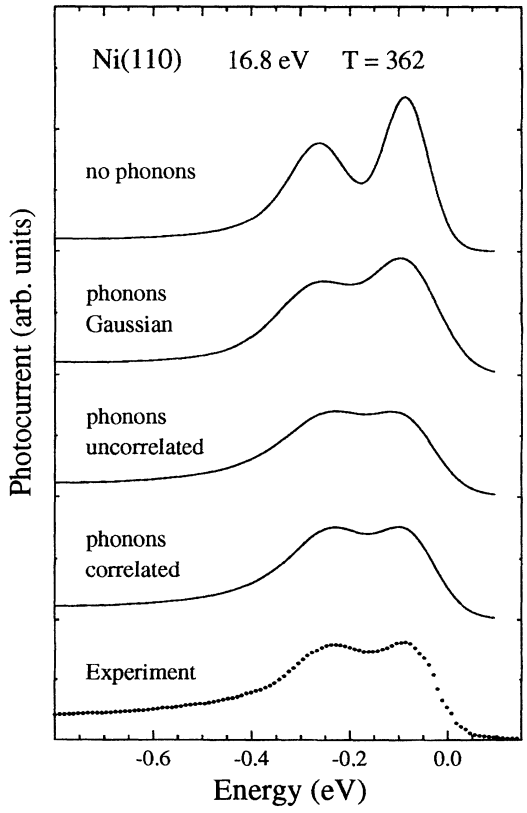

FIG. 5. *Spin-integrated* normal photoemission from Ni(110) at $T = 362$ K: experiment (dotted curve) and theory (solid curves) including spin fluctuations and no phonons as well as phonons treated as indicated.

between about 6 and 14 Å. For ferromagnets with larger exchange splittings, the manifestation of local magnetic properties near T_c in photoemission spectra is expected to be more weakly masked by phonon effects than in the present case of Ni.

ACKNOWLEDGMENTS

This work was funded by the German DAAD and by the Mexican CONACyT.

*Present address: Depto. de Fisica, Centro de Investigacion y de Estudios Avanzados del IPN, Apdo. Postal 14-740, 07000 Mexico, D.F.

[1]R. Feder, in *Polarized Electrons in Surface Physics*, edited by R. Feder (World Scientific, Singapore, 1985), Chap. 4; R. Clausberg and R. Feder, *ibid.*, Chap. 14.
[2]H. Gollisch and R. Feder, Physica B **161**, 169 (1989); Solid State Commun. **76**, 76 (1990).
[3]E.M. Haines, V. Heine, and A. Ziegler, J. Phys. F **16**, 1343 (1986).
[4]H. Gollisch and R. Feder, Solid State Commun. **84**, 537 (1992).
[5]J. Braun, G. Borstel, and W. Nolting, Phys. Rev. B **46**, 3510 (1992).
[6]I. Delgadillo, H. Gollisch, and R. Feder, Solid State Commun. **88**, 789 (1993).
[7]J.S. Slater and G.F. Koster, Phys. Rev. **94**, 1498 (1954).
[8]R.R. Sharma, Phys. Rev. B **19**, 2813 (1979).
[9]W.A. Harrison, *Electronic Structure and the Properties of Solids* (Freeman and Co., San Francisco, 1980).
[10]R. Haydock, in *Solid State Physics: Advances in Research and Applications*, edited by F. Seitz, D. Turnbull, and H. Ehrenreich (Academic Press, New York, 1980), Vol. 35.
[11]R. McLean and R. Haydock, J. Phys. C **10**, 1929 (1977).
[12]*Numerical Data and Functional Relationships in Science and Technology*, edited by K.-H. Hellwege and A. M. Hellwege, Landolt-Börnstein, Group III, Vol. 1, New Series (Springer, Berlin, 1966).
[13]R. Raue, H. Hopster, and R. Clauberg, Z. Phys. B **54**, 121 (1984).
[14]J. Würtenberg, Ph.D. dissertation, Universität Frankfurt, 1987.